Regional moisture balance control of landslide motion: Implications for landslide forecasting in a changing climate

Jeffrey A. Coe
U.S. Geological Survey, Denver Federal Center, MS 966, Denver, Colorado 80225, USA

ABSTRACT

I correlated 12 years of annual movement of 18 points on a large, continuously moving, deep-seated landslide with a regional moisture balance index (moisture balance drought index, MBDI). I used MBDI values calculated from a combination of historical precipitation and air temperature data from A.D. 1895 to 2010, and downscaled climate projections using the Intergovernmental Panel on Climate Change A2 emissions scenario for 2011–2099. At the landslide, temperature is projected to increase ~0.5 °C/10 yr between 2011 and 2099, while precipitation decreases at a rate of ~2 mm/10 yr. Landslide movement correlated with the MBDI with integration periods of 12 and 48 months. The correlation between movement and MBDI suggests that the MBDI functions as a proxy for groundwater pore pressures and landslide mobility. I used the correlation to forecast decreasing landslide movement between 2011 and 2099, with the head of the landslide expected to stop moving in the mid-21st century. The MBDI, or a similar moisture balance index that accounts for evapotranspiration, has considerable potential as a tool for forecasting the magnitude of ongoing deep-seated landslide movement, and for assessing the onset or likelihood of regional, deep-seated landslide activity.

INTRODUCTION

How will active and dormant landslides respond to climate change? This is a challenging question for Earth scientists (e.g., Sidle, 2007; Briceno et al., 2007; Crozier, 2010; Winter et al., 2010) that has broad implications for population centers throughout the world. There are multiple issues that make this question difficult to answer, but two issues are prominent. First, landslide activity is difficult to forecast in a static climate (e.g., van Westen et al., 2006), so attempting to forecast activity in a changing climate seems challenging at best. Second, projections of future precipitation based on simulations from climate models tend to be available as monthly or annual precipitation for large areas, rather than as precipitation frequency, duration, and intensity at individual sites.

The responsiveness of individual landslides to precipitation is dependent on their geometry; stratigraphic, structural, and hydraulic properties; soil moisture and groundwater characteristics; and the frequency, duration, and intensity of precipitation (e.g., van Asch et al., 1999). Large, deep-seated (>5 m in thickness), slow-moving landslides typically have complex boundaries, distinct kinematic elements, and materials with hydraulic conductivities of <10^{-4} m/s and diffusivities <10^{-4} m^2/s (e.g., Iverson and Major, 1987; Baum and Reid, 1995; Schulz et al., 2009a; Calabro et al., 2010). The properties of deep-seated landslides make the timing of their movement with respect to precipitation complex; some landslides respond days after precipitation (Baum and Reid, 1995) and others respond weeks to months after precipitation (e.g., Iverson and Major, 1987). The magnitude of movement during each movement episode is dependent on pore pressures at basal shear surfaces, pressures that are functions of groundwater flow and propagating pressure waves from long-term precipitation integrated over time periods of weeks to months. Because long-term precipitation patterns are readily available from downscaled climate projections, the effects of climate change on landslide motion may be easier to forecast for deep-seated landslides than for shallow landslides, which are highly sensitive to individual precipitation events. This situation highlights a need for landslide forecasting tools that account for long-term moisture and groundwater conditions.

In this paper, I correlated a regional moisture balance index with 12 yr of annual movement data (1998–2010) from the deep-seated Slumgullion landslide in the San Juan Mountains of Colorado (United States). The moisture balance index, called the moisture balance drought index (MBDI; Ellis et al., 2010; http://azclimate.asu.edu/mbdi/index.php), is computed from monthly air temperature and precipitation values for all 2.5 min (~4 km, 16 km^2) cells within the 634,550 km^2 Colorado River Basin. I used MBDI values computed from a combination of historical (1895–2010) and projected (2011–2099) monthly values at the head of the landslide. During the 12 yr landslide monitoring period, MBDI values at Slumgullion were near historical highs and lows. Thus, the 12 yr period captured a broad range of historical landslide behavior. I used the correlation between landslide movement and MBDI values to forecast landslide movement between 2011 and 2099.

SLUMGULLION LANDSLIDE

The Slumgullion landslide (Fig. 1; Fig. DR1 in the GSA Data Repository[1]) is in the montane and subalpine ecological zones of the San Juan Mountains in southwestern Colorado. Vegetation on the landslide consists of sparse, open stands of conifer and aspen trees. The active part of the landslide (Fig. 1) ranges in elevation from ~2950 to 3650 m, has an estimated volume of ~20×10^6 m^3 (Parise and Guzzi, 1992), saturated hydraulic conductivities of 1.53×10^{-5} to 4.26×10^{-6} m/s (Schulz et al., 2009b), and an estimated hydraulic diffusivity of 7.8×10^{-5} m^2/s (Schulz et al., 2009a). The depth of the basal shear surface is unknown, but Parise and Guzzi (1992) estimated an average depth of 13 m and Schulz et al. (2009a) estimated a depth of 20 m at the landslide toe. Annual rates of movement range from ~15 cm/yr at the head of the landslide, to 1.5 m/yr at the toe,

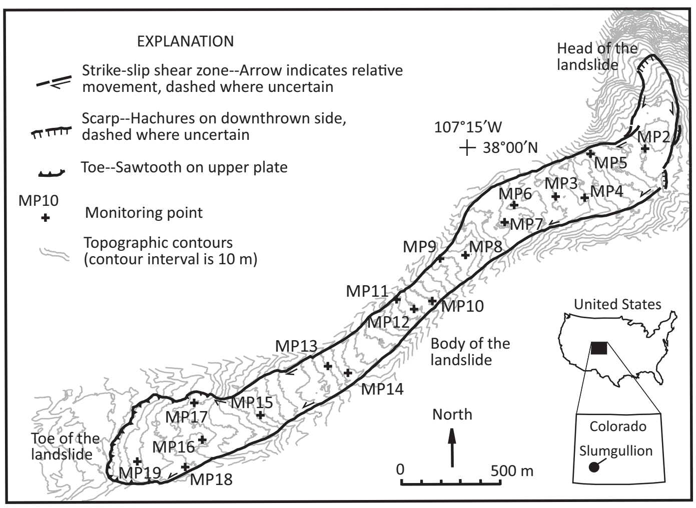

Figure 1. Map of active part of Slumgullion landslide (inset shows location of landslide within Colorado). Landslide border is from Fleming et al. (1999).

[1]GSA Data Repository item 2012091, Figures DR1–DR3 and Tables DR1 and DR2, is available online at www.geosociety.org/pubs/ft2012.htm, or on request from editing@geosociety.org or Documents Secretary, GSA, P.O. Box 9140, Boulder, CO 80301, USA.

© 2012 Geological Society of America. For permission to copy, contact Copyright Permissions, GSA, or editing@geosociety.org.

to 7 m/yr in the body of the landslide (Fleming et al., 1999; Coe et al., 2003). Schulz et al. (2009a) found that individual episodes of movement correlated with low-pressure atmospheric tides. Modeling by Schulz et al. (2009a) indicated that tides cause upward fluid flow within the landslide, thus reducing landslide shear strength and triggering movement.

METHODS

Global Positioning System Surveys

I used rapid-static GPS surveying with relative positioning to survey 18 monitoring points (MP) on the landslide (Fig. 1) during 12 summer field campaigns of 1 to 2 days between 1998 and 2010. GPS surveys were conducted once each summer, except 2005, when no survey was done. The 18 monitoring points were distributed across the active landslide (Fig. 1). There was no snow on the landslide during any of the campaigns. The time periods between survey campaigns were not exact annual periods (i.e., not exactly 365 days; Table DR1 in the Data Repository), therefore mean daily horizontal movement (mm/day) between surveys was used for correlation with MBDI values.

Regional Moisture Balance Index

The MBDI is a representation of moisture balance conditions at a given location at a given point in time. The MBDI is based on monthly precipitation (*P*, mm/month) minus monthly potential evapotranspiration (*PE*, mm/month), where *PE* is an estimate of the amount of water removed from the land surface through evaporation and transpiration assuming an unlimited water supply (Ellis et al., 2010). Ellis et al. (2010) determined *PE* using the equation

$$PE = 13.97 d D^2 W_t, \quad (1)$$

where d is the number of days in a month, D is the mean monthly hours of daylight in units of 12 h, and W_t is a saturated water-vapor term calculated as

$$W_t = \frac{4.95 e^{0.062T}}{100}, \quad (2)$$

where T is mean monthly air temperature (°C).

From a time series of monthly $P - PE$ values, aggregates of $P - PE$ are calculated for a variety of preceding time periods (herein called integration periods; Fig. DR2). Individual MBDI values are percentile rankings (0–100) of aggregated $P - PE$ values relative to a period of record. For example, an MBDI value for June 2010 with a 6 month integration period is a percentile ranking of $P - PE$ for January 2010 through June 2010 based on a comparison with $P - PE$ for every January to June period in the period of record.

To determine the appropriate integration periods, I estimated the response time for slope-normal pore pressure transmission from the ground surface to the basal shear surface using an estimated landslide thickness (H) of 5–30 m and an estimated hydraulic diffusivity (D_0) of 7.8×10^{-5} m^2/s (Schulz et al., 2009a) in the time scale approximation H^2/D_0 of Iverson (2000). The estimated response times ranged from ~1 to 44 months. To account for this possible range in response times, I used MBDI values with 1–48 month integration periods. These MBDI values were calculated from combined historical and projected T and P between 1895 and 2099.

The T and P values came from two sources: the parameter-elevation regressions on independent slopes model (PRISM; Daly et al., 1994) by the PRISM Climate Group at Oregon State University, and downscaled climate projections from the U.S. Bureau of Reclamation, Lawrence Livermore National Labs, Santa Clara University, and Climate Central (Maurer et al., 2007). PRISM distributes weather station measurements of T and P to 2.5 min (~4 km) grid cells in the continental U.S. and is designed to account for orographic precipitation in complex mountainous terrain by using localized precipitation-elevation relations. I used T and P from the PRISM cell at the head of the active landslide for the period 1895–2010.

Downscaled projections consisted of 36 projections from 16 climate models forced using the Intergovernmental Panel on Climate Change A2 emissions scenario (Fig. DR3). A2 is a scenario of relatively high emissions of carbon dioxide and other greenhouse gases that assumes a future world of continuously increasing population and independently operating nations (Nakicenvoic et al., 2000). I selected the A2 scenario because the current trajectory of emissions corresponds with a high emissions scenario. Projections were downscaled to ~12 km grid cells for continental U.S. using the statistical technique described by Wood et al. (2004). Original projections were from the World Climate Research Programme's Coupled Model Intercomparison Project Phase 3 (CMIP3) multimodel data set (Meehl et al., 2007).

I calculated T and P for the period 2011–2099 by taking the mean of the 36 projections for the single 12 km grid cell that incorporated the entire active landslide. I calculated mean annual MBDI values using monthly MBDI values with 1–48 month integration periods for each period between GPS surveys. I used regression analyses to correlate mean annual MBDI values to mean daily landslide movement (per year) at the 18 monitoring points.

RESULTS

All monitoring points moved between each GPS survey (Fig. 2). Cumulative horizontal movement over the monitoring period ranged from 2 to 4 m at MP2 and MP17 at the head and toe of the landslide, respectively, to ~58 m at MP12 in the body of the landslide (Fig. 2A). The trend of mean daily horizontal movement decreased during the monitoring period (Fig. 2B).

Mean annual MBDI was near historical highs between 1998 and 2001, and near historical lows between 2002 and 2006 (Fig. 3), and is projected to decrease between 2011 and 2099. MBDI in this period is less variable than historical MBDI data (pre-2011 data on the left side of Fig. 3) because it is derived from the mean values of T and P from 36 projections. Averaging removes the variability that is observed in both pre-2011 data, and in individual projections. The projected decrease in MBDI between 2011 and 2099 is caused primarily by a steady increase in T. This projected increase is ~0.5 °C/10 yr or 0.05 °C/yr, which is less than indicated by recent observational evidence in the San Juan Mountains (1 °C/10 yr between 1990 and 2005; Rangwala and Miller, 2010).

Regression analyses of mean daily landslide movement and mean annual MBDI yields r^2 values that ranged from 0.59 to 0.94 (Fig. 4). Mean daily movement of the upper part of the landslide (Fig. 1) and the toe was best modeled by mean annual MBDI with a 12 month integration period (Fig. 4). Mean daily movement of the body of the landslide was best modeled by mean annual MBDI values with a 48 month integration period.

Figure 5 shows the forecast mean daily movement of landslide points based on the mean annual MBDI between 2011 and 2099 (Fig. 3) and the regression equations in Table DR2. The long-term trend of daily movement is projected to decrease for all parts of the landslide. This forecast suggests that the head of the landslide (point MP2, Fig. 5) will stop moving ca. A.D. 2060. Because of the averaged T and P data used to calculate MBDI, the landslide movement forecast does not account for all of the variability in movement caused by extremely wet and dry years. However, the overall forecast trend of decreasing landslide movement is consistent with Rangwala and Miller's (2010) observations of increasing temperatures between 1990 and 2005, as well as GPS observations showing decreasing movement between 1998 and 2010 (Fig. 2B).

IMPLICATIONS AND CONCLUSIONS

Results from this study have implications for ongoing activity at Slumgullion, and for general landslide forecasting in a changing climate. For Slumgullion, results indicate that a regional moisture balance index can function as a proxy for basal groundwater pore pressures and landslide mobility. The MBDI is a good predictor of the magnitude of

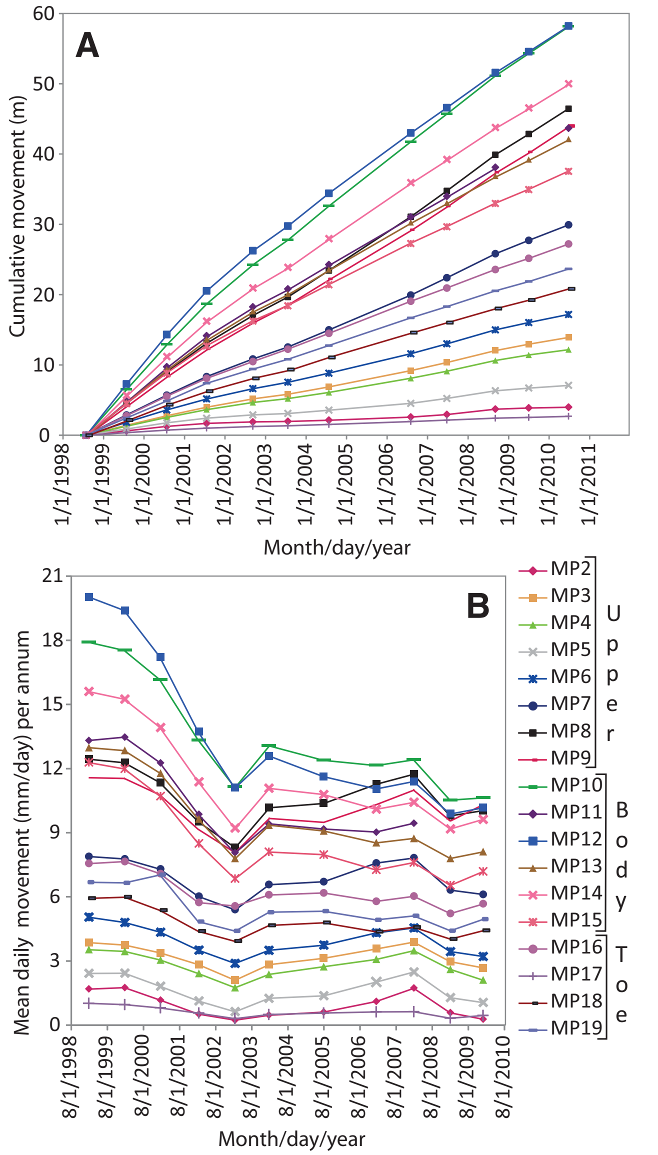

Figure 2. Landslide movement data for 18 points on the landslide. A: Cumulative movement for 12 yr monitoring period. Monitoring points (MP) are plotted at ending dates of global positioning system surveys. B: Mean daily movement for each annual period. Points are plotted at mid-points between survey dates. MP11 was not surveyed in 2009.

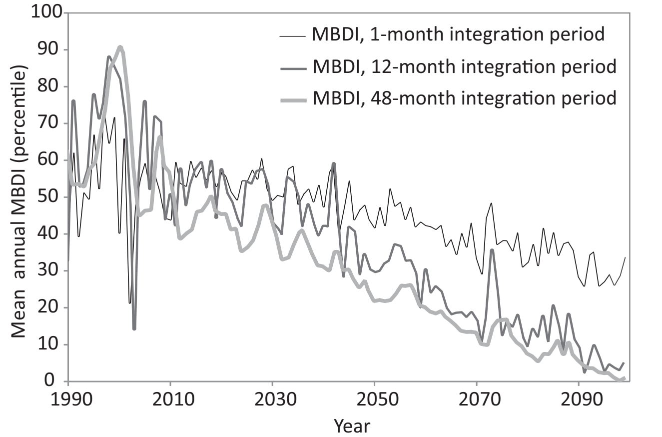

Figure 3. Diagram showing mean annual moisture balance drought index (MBDI) calculated from combined historical and projected temperature and precipitation data. Warmest and/or driest periods have low MBDI values, and coolest and/or wettest periods have high MBDI values.

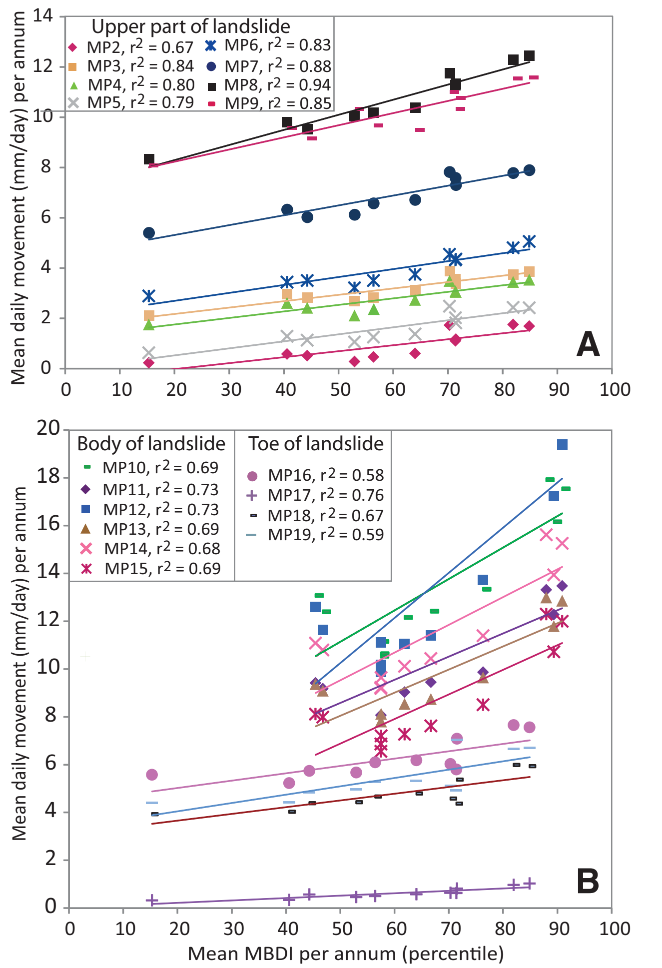

Figure 4. Diagram showing best-fit regression lines for correlations of mean daily movement and mean annual moisture balance drought index (MBDI) for each period between global positioning system surveys. Integration periods used were 12 months for monitoring points MP2–MP9 and MP16–MP19, and 48 months for MP10–MP15. The r^2 values for each line are shown. See Table DR2 (see footnote 1) for standard errors of regressions. A: Monitoring points on upper half of landslide. B: Monitoring points on lower half of landslide.

movement for all parts of the landslide. Moisture balance conditions measured at moderately long periods of time of 12 and 48 months control the magnitude of mean daily movement. Differences in MBDI integration periods for the slow-moving head and toe of the landslide (12 months) and fast-moving body of the landslide (48 months) are probably related to differences in landslide width (i.e., constricted width of the landslide body relative to the head and toe regions). This difference in width probably affects landslide thickness and hydraulic properties, which influence groundwater flow and pore-pressure transmission.

Over the next 90 yr, landslide movement is expected to gradually decrease (Fig. 5), with the head of the landslide projected to stop moving before other parts of the landslide. Although this forecast is based on projections using a relatively high emissions scenario, results suggest that even if air temperatures were to increase by only half as much as projected, movement of Slumgullion will still decrease. In addition to uncertainties in projections of temperature and precipitation, other vari-

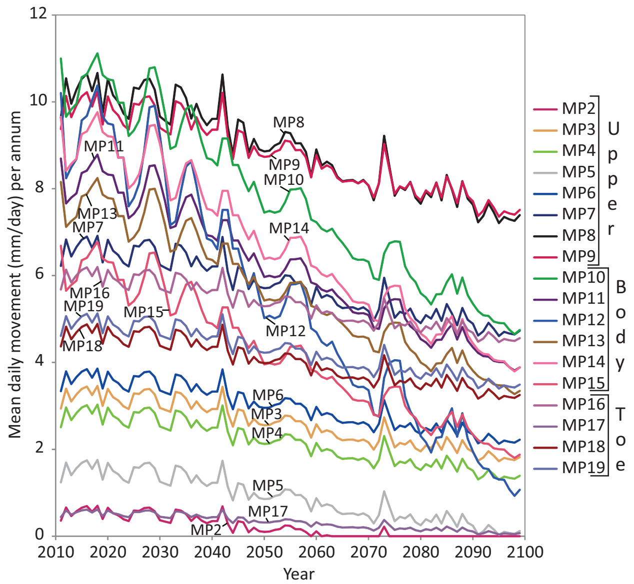

Figure 5. Forecast movement of landslide monitoring points (MP) based on annual moisture balance drought index data shown in Figure 3. Standard errors of predicted movement range from ±0.2 to ±0.4 mm/day for upper part of landslide, ±1.1 to ±2.0 mm/day for body, and ±0.1 to ±0.6 mm/day for toe.

ables could adversely affect my forecast of decreasing movement. These variables include extensive changes in vegetation, resupply of material to the landslide by large failures of the headscarp, and changes in landslide kinematic elements and dynamics.

Even with these uncertainties, the strong correlation between the relatively simple, regionally based MBDI and movement of the complex landslide has significant implications for forecasting changes to ongoing deep-seated landslide movement, and new or recurring movement based on projected climatic changes. First, the projected decrease in movement at Slumgullion highlights the point that in a warming climate, assessments of future landslide activity should incorporate changes in both precipitation and evapotranspiration. Second, regionally based moisture balance indices have potential to improve or extend forecasts of landslide activity based on field monitoring. In an ideal forecasting situation, groundwater pore pressures and movement of a large number of deep-seated landslides would be monitored with field instrumentation for long periods of time (>3 yr) to develop specific groundwater pressure thresholds for the onset of deep-seated landslide activity. However, in reality, very few deep-seated landslides are monitored for the periods of time needed to develop groundwater thresholds. Thus, a landslide activity threshold based on a regional moisture balance index would be a very useful forecasting tool.

ACKNOWLEDGMENTS

I thank Andrew Ellis at Arizona State University for providing moisture balance drought index data; Jonathan Godt, Bill Ellis, Bill Savage, and many others who assisted with global positioning system surveys from 1998 to 2001; Bill Schulz and Jonathan Godt for helpful discussions; Gary Clow, Bill Schulz, Rex Baum, and three anonymous reviewers for constructive reviews; and the Program for Climate Model Diagnosis and Intercomparison, the World Climate Research Programme's Working Group on Coupled Modeling, and the U.S. Department of Energy for making available the CMIP3 (Coupled Model Intercomparison Project) data set.

REFERENCES CITED

Baum, R.L., and Reid, M.E., 1995, Geology, hydrology, and mechanics of a slow-moving, clay-rich landslide, Honolulu, Hawaii, *in* Haneberg, W.C., and Anderson, S.A., eds., Clay and shale slope instability: Geological Society of America Reviews in Engineering Geology, v. X, p. 79–105.

Briceno, S., Basabe, P., and Bonnard, C., 2007, Landslides and climate change: A world perspective, but a complex question, *in* McInnes, R., et al., eds., Landslides and climate change: Challenges and solutions: London, Taylor & Francis, p. 3–6.

Calabro, M.D., Schmidt, D.A., and Roering, J.J., 2010, An examination of seasonal deformation at the Portuguese Bend landslide, southern California, using radar interferometry: Journal of Geophysical Research, v. 115, F02020, doi:10.1029/2009JF001314.

Coe, J.A., Ellis, W.L., Godt, J.W., Savage, W.Z., Savage, J.E., Michael, J.A., Kibler, J.D., Powers, P.S., Lidke, D.J., and Debray, S., 2003, Seasonal movement of the Slumgullion landslide determined from global positioning system surveys and field instrumentation, July 1998–March 2002: Engineering Geology, v. 68, p. 67–101, doi:10.1016/S0013-7952(02)00199-0.

Crozier, M.J., 2010, Deciphering the effect of climate change on landslide activity: A review: Geomorphology, v. 124, p. 260–267, doi:10.1016/j.geomorph.2010.04.009.

Daly, C., Neilson, P., and Phillips, D.L., 1994, A statistical-topographical model for mapping climatological precipitation over mountainous terrain: Journal of Applied Meteorology, v. 33, p. 140–158, doi:10.1175/1520-0450(1994)033<0140:ASTMFM>2.0.CO;2.

Ellis, A.W., Goodrich, G.B., and Garfin, G.M., 2010, A hydroclimatic index for examining patterns of drought in the Colorado River Basin: International Journal of Climatology, v. 30, p. 236–255, doi:10.1002/joc.1882.

Fleming, R.W., Baum, R.L., and Giardino, M., 1999, Map and description of the active part of the Slumgullion landslide, Hinsdale County, Colorado: U.S. Geological Survey Miscellaneous Investigation Series Map I-2672, http://pubs.usgs.gov/imap/i-2672/.

Iverson, R.M., 2000, Landslide triggering by rain infiltration: Water Resources Research, v. 36, p. 1897–1910, doi:10.1029/2000WR900090.

Iverson, R.M., and Major, J.J., 1987, Rainfall, ground-water flow, and seasonal movement at Minor Creek landslide, northwestern California: Physical interpretation of empirical relations: Geological Society of America Bulletin, v. 99, p. 579–594, doi:10.1130/0016-7606(1987)99<579:RGFASM>2.0.CO;2.

Maurer, E.P., Brekke, L., Pruitt, T., and Duffy, P.B., 2007, Fine-resolution climate projections enhance regional climate change impact studies: Eos (Transactions, American Geophysical Union), v. 88, no. 47, p. 504, doi:10.1029/2007EO470006.

Meehl, G.A., and 13 others, 2007, Global climate projections, *in* Solomon, S., et al., eds., Climate change 2007: The physical science basis. Contribution of Working Group I to the Fourth Assessment Report of the Intergovernmental Panel on Climate Change: Cambridge, UK, and New York, Cambridge University Press, p. 747–845.

Nakicenvoic, N., and 14 others, 2000, Special report on emissions scenarios: A special report of Working Group III of the Intergovernmental Panel on Climate Change: Cambridge, UK, Cambridge University Press, 599 p.

Parise, M., and Guzzi, R., 1992, Volume and shape of the active and inactive parts of the Slumgullion landslide, Hinsdale County, Colorado: U.S. Geological Survey Open-File Report 92–216, 29 p., http://pubs.usgs.gov/of/1992/0216/.

Rangwala, I., and Miller, J.R., 2010, Twentieth century temperature trends in Colorado's San Juan Mountains: Arctic, Antarctic, and Alpine Research, v. 42, no. 1, p. 89–97, doi:10.1657/1938-4246-42.1.89.

Schulz, W.H., Kean, J.W., and Wang, G., 2009a, Landslide movement in southwest Colorado triggered by atmospheric tides: Nature Geoscience, v. 2, p. 863–866, doi:10.1038/ngeo659.

Schulz, W.H., McKenna, J.P., Kibler, J.D., and Biavati, G., 2009b, Relations between hydrology and velocity of a continuously moving landslide—Evidence of pore-pressure feedback regulating landslide motion?: Landslides, v. 6, p. 181–190, doi:10.1007/s10346-009-0157-4.

Sidle, R.C., 2007, Using weather and climate information for landslide prevention and mitigation, *in* Sivakumar, M.V.K., and Ndiang'ui, N., eds., Climate and land degradation: Berlin, Springer, p. 285–307.

van Asch, T.W.J., Buma, J., and van Beek, L.P.H., 1999, A view on some hydrological triggering systems in landslides: Geomorphology, v. 30, p. 25–32, doi:10.1016/S0169-555X(99)00042-2.

van Westen, C.J., van Asch, T.W.J., and Soeters, R., 2006, Landslide hazard and risk zonation—Why is it still so difficult?: Bulletin of Engineering Geology and the Environment, v. 65, p. 167–184, doi:10.1007/s10064-005-0023-0.

Winter, M.G., Dixon, N., Wasowski, J., and Dijkstra, T.A., 2010, Introduction to land-use and climate change impacts on landslides: Quarterly Journal of Engineering Geology and Hydrology, v. 43, p. 367–370, doi:10.1144/1470-9236/10-035.

Wood, A.W., Leung, L.R., Sridhar, V., and Lettenmaier, D.P., 2004, Hydrologic implications of dynamical and statistical approaches to downscaling climate model outputs: Climatic Change, v. 62, p. 189–216, doi:10.1023/B:CLIM.0000013685.99609.9e.

Manuscript received 6 October 2011
Revised manuscript received 1 November 2011
Manuscript accepted 6 November 2011

Printed in USA